

Peering Deeper into the Plerionic Supernova Remnant G21.5–0.9

Benson Guest and Samar Safi-Harb¹

¹ Department of Physics and Astronomy, University of Manitoba, Winnipeg, Manitoba, R3T 2N2, Canada

Abstract

The supernova remnant (SNR) G21.5–0.9 has been observed regularly with the *Chandra* X-ray observatory since its launch in 1999, and has become a textbook example for a young plerionic SNR. The remnant hosts a bright pulsar wind nebula (PWN), powered by a 61.8 ms pulsar (PSR J1833–1034, $B=3.6\times 10^{12}$ G, and spin down luminosity $\dot{E}=3.3\times 10^{37}$ erg s⁻¹), and a faint limb-brightened shell revealed in X-rays with *Chandra*. The nature of the X-ray emission from the shell (thermal versus non-thermal) and knots within the nebula (ejecta?) remains a puzzle. To address this, we present a follow-up X-ray analysis of G21.5–0.9 (study in progress) utilizing the deepest (> 1 Msec total) exposure to date, including ~ 780 ks with the Advanced CCD Imaging Spectrometer (ACIS) and ~ 310 ks with the High Resolution Camera (HRC). These observations spanning ~ 15 years also allow for the study of variability and tracking the motion of small-scale structures within the PWN.

1 Introduction

G21.5–0.9 has become a textbook example for a plerionic SNR (Gaensler & Slane 2006, Matheson & Safi-Harb 2005). Being a calibration target for *Chandra*, it has been observed since *Chandra*'s launch in 1999. Earlier *Chandra* observations have been reported in Slane et al. (2000), Safi-Harb et al. (2001), Matheson & Safi-Harb (2005), Bocchino et al. (2006), Matheson & Safi-Harb (2010). One of the surprises *Chandra* brought was the discovery of an extended halo (that extends well beyond the known bright pulsar wind nebula) with knots to the north (also known as the northern ‘spur’), as well as limb brightening to the east. The pulsar has been discovered at radio wavelengths (Gupta et al. 2005; Camilo et al. 2006). Here we present preliminary results from all calibration observations extending from 1999 up to 2014, accumulating over 1 Msec of effective exposure time. The goal of this study is to address outstanding questions on the nature of the X-ray emission from the different components of this composite system. These observations spanning ~ 15 years also allow for the study of variability and tracking the motion of small-scale structures within the PWN. A more detailed analysis and discussion will be presented in a forthcoming publication.

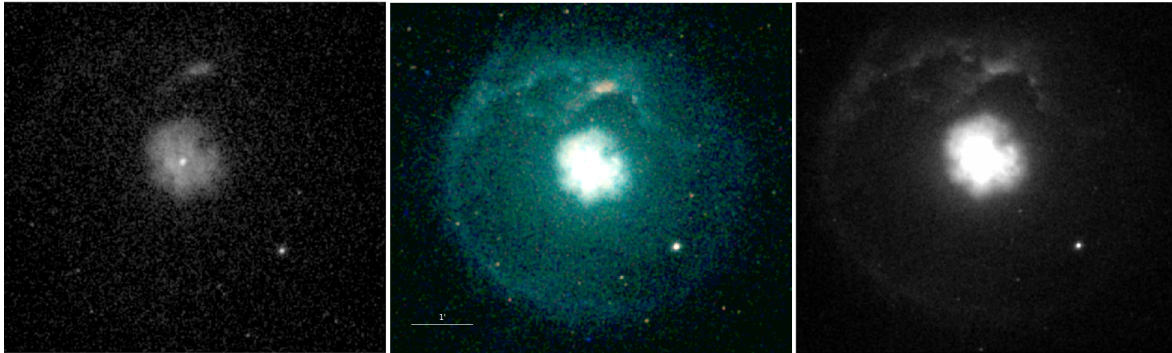


Figure 1: Chandra ACIS images of G21.5–0.9 with an effective exposure of 786 ks. Centre: RGB image coloured as follows; Red: 0.5–1.2 keV, Green: 1.2–2 keV, Blue: 2–7 keV. Left and Right: 0.5–1.2 keV and 1.2–10 keV, respectively.

2 Neutron Star

Emission from the neutron star was studied using only observations with an off-axis angle less than $3'$. 90% of the energy of a point source at 1.5 keV is contained within a $1.5''$ radius, therefore a circular region with $2''$ radius centred at $\alpha(2000) = 18^h33^m33^s.54$, $\delta(2000) = -10^\circ34'07''.6$ was used to extract the neutron star's spectrum. Background spectra were extracted from a $2''$ – $4''$ annulus centred on the same coordinates. The spectra were fit with an absorbed power-law model with the column density frozen at $2.32 \times 10^{22} \text{ cm}^{-2}$, the value found from fitting the entire PWN. This was then compared with the result of fitting to an absorbed power-law + blackbody model. The power-law model alone is characterized by a spectral index of $\Gamma = 1.58 \pm 0.02$ with $\chi^2_\nu(\nu) = 1.33(1423)$ while the power-law + blackbody model has a steeper index $\Gamma = 1.39 \pm 0.11$ with temperature $kT = 0.43$ (0.33 – 0.47) keV and $\chi^2_\nu(\nu) = 1.32(1421)$. The addition of a thermal component which accounts for $\sim 10\%$ of the flux improves the fit slightly with an F-test probability of 0.02. This suggests the thermal emission is less statistically significant than that found in previous work with less total exposure (Matheson & Safi-Harb 2010).

3 Northern Knot

The northern knot (or northern ‘spur’) stands out as a region of enhanced soft X-ray emission to the north of the PWN (see Fig. 1). A pure thermal plasma model fit (*vpshock* in XSPEC) is characterized by a temperature of $kT = 3.5 \pm 0.2$ keV, sub-solar abundances of Mg (0.47 ± 0.06), Si (0.20 ± 0.05) and S (0.01 ; < 0.66) and an ionization timescale of $9.4 \pm 1.1 \times 10^9 \text{ cm}^{-3} \text{ s}$. While the fit is acceptable ($\chi^2_\nu(\nu) = 1.08(1459)$), previous *Chandra* and *XMM-Newton* observations (Matheson & Safi-Harb 2010; Bocchino et al. 2006) were unable to favour thermal over non-thermal, while observations with NuSTAR (Nynka et al 2014) detected enhanced emission above 10 keV suggesting the presence of a non-thermal component. The results of the thermal + non-thermal model fit are outlined in Table 1.

Γ	2.26 (2.17 – 2.35)
Norm (10^{-4} keV $^{-1}$ cm $^{-2}$ s $^{-1}$)	2.29 (2.02 – 2.56)
kT (keV)	0.17 (0.14 – 0.24)
Mg	0.57 (0.29 – 1.19)
Si	1.68 (0.83 – 4.0)
S	7.6 (< 41)
n_{et} (10^{11} cm $^{-3}$ s)	5.7 (2–51)
Norm (10^{-2} cm $^{-2}$)	4.2 (1.1 – 13)
χ^2_ν	1.02 (1457)

Table 1: Two component power-law + vpshock model fit to the northern knot spectra with the column density frozen at 2.32×10^{22} cm $^{-2}$, the best fit value for the PWN. The ranges shown are 2σ .

We find enhanced abundances for Silicon and Sulfur which supports the scenario that the knots contain shock-heated ejecta. We note however that the abundances are not very well constrained.

4 Eastern Limb

To date, no radio emission has been detected from the SNR shell (Bietenholz et al. 2011). As mentioned, the eastern limb was first revealed in X-rays in previous studies. However its nature as either thermal or non-thermal was not confirmed. With the additional data our best fit is found from a two component power-law + pshock model characterized by a spectral index $\Gamma = 2.43 \pm 0.06$, temperature $kT = 0.21$ (0.15 – 0.28) keV and a low ionization timescale $n_{et} = 2.42$ (<4.97) $\times 10^9$ cm $^{-3}$ s with $\chi^2_\nu(\nu) = 0.95$ (3157). The emission is primarily non-thermal with the thermal component contributing only a few % of the total flux.

5 Variability

Observations of other PWNe have revealed structures which appear and move on timescales of weeks with velocities of $\sim 0.5c$ (Pavlov et al. 2001). With 15 years of Chandra observations, we are able to examine changes on different timescales. Figure 1 shows ACIS observations which have been normalized to 20 ks exposures. Knots of enhanced emission are observed to form and move outwards from the central pulsar. Difference images were used to look for possible motion of these knots. Assuming knots which appear as a region of enhanced emission radially outward from a region lacking emission in a difference image are the same knot which moved between observations, we identify velocities of these knots on the order of $0.2 - 0.7c$.

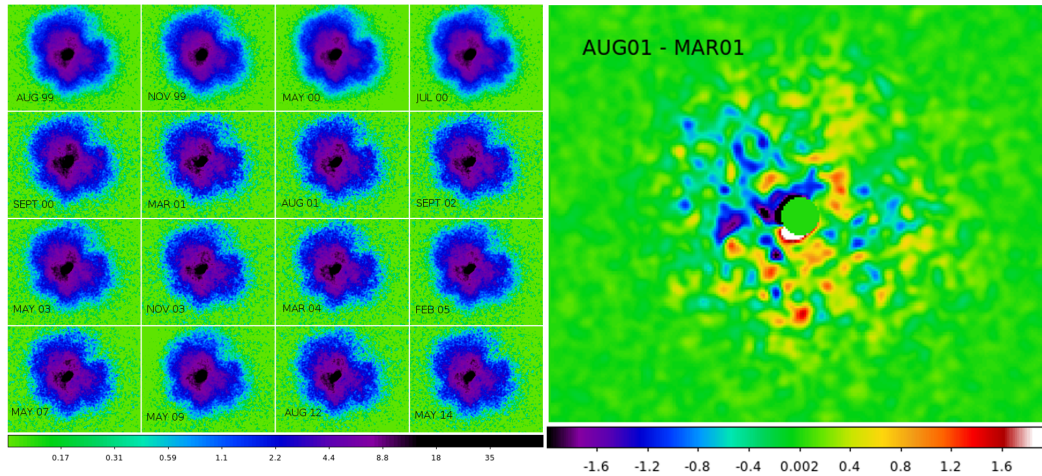


Figure 2: Left: ACIS observations normalized to 20 ks. Note the knots of emission which appear near the pulsar and propagate outwards Right: Difference image generated by subtracting the March 2001 observations from the August 2001 observations with each normalized to a single 20 ks exposure. The pulsar has been removed to better display the variability.

Acknowledgments

This research was primarily supported by the Natural Sciences and Engineering Research Council of Canada (NSERC).

References

- Bietenholz, Matheson, H., Safi-Harb, S., Brogan, C., & Bartel, N. 2011, *MNRAS*, 412, 1221.
 Matheson, H. & Safi-Harb, S. 2010, *ApJ*, 724, 572.
 Gupta, Y., Mitra, D., Green, D. A., & Acharya, A. 2005, *CSci*, 89, 853.
 Camilo, F., Ransom, S. M., Gaensler, B. M. et al. 2006, *ApJ*, 637, 456.
 Bocchino, F., van der Swaluw, E., Chevalier, R. & Bandiera, R. 2005, *A&A*, 442, 539.
 Matheson, H. & Safi-Harb, S. 2005, *AdSpR*, 35, 1099.
 Safi-Harb, S., Harrus, I. M., Petre, R., Pavlov, G. G., Koptsevich, A. B., & Sanwal, D. 2001, *ApJ*, 561, 308.
 Slane, P. O., Chen, Y., Schulz, N. S., Seward, F. D., Hughes, J. P., & Gaensler, B. M. 2000, *ApJ*, 533, L29.
 Nynka, M., Hailey, C. J., Reynolds, S. P. et al. 2014, *ApJ*, 789, 72N.
 Pavlov, G. G., Kargaltsev, O. Y., Sanwal, D., Garmire, G. P. 2001, *ApJ*, 554, L189.